



# Quantification of Mitochondrial Network Characteristics in Health and Disease

# 10

Andrew J. Valente, Joao Fonseca,  
Fereshteh Moradi, Gregory Foran,  
Alexander Necakov, and Jeffrey A. Stuart

## Abstract

The term ‘mitochondrial dynamics’ is commonly used to refer to ongoing fusion and fission of mitochondrial structures within a living cell. A growing number of diseases, from Charcot Marie Tooth Type 2a neuropathies to cancer, is known to be associated with the dysregulation of mitochondrial dynamics, leading to irregularities of mitochondrial network morphology that are associated with aberrant metabolism and cellular dysfunction. Studying these phenomena, and potential pharmacological interventions to correct them, in cultured cells is a powerful approach to developing treatments or cures. Appropriately designed experiments and quantitative approaches for characterizing mitochondrial morphology and function are essential for furthering our understanding. In this chapter, we discuss the importance of cell incubation conditions, choices around imaging modalities, and data analysis tools with respect to experimental outcomes and the interpretation of results from studies of mitochondrial dynamics. We focus primarily on the quantitative analysis of mitochondrial morphology, providing an overview of the

available tools and approaches currently being used and discussing some of the strengths and weaknesses associated with each. Finally, we discuss how the ongoing development of imaging and analysis tools continues to improve our ability to study normal and aberrant mitochondrial physiology in vitro and in vivo.

## Keywords

MiNA · Mitochondrial networks · Mitochondrial dynamics · Fusion · Fission · Cell physiology · Live cell imaging

## 10.1 Introduction

In all nucleated animal cells, even post-mitotic terminally differentiated cells like neurons and myofibres, mitochondria are in a dynamic state of ongoing biogenesis, involving replication of mitochondrial DNA (mtDNA) and gain of mitochondrial mass, and mitophagy involving mtDNA degradation and loss of mitochondrial mass. Although these are clearly dynamic processes, the term ‘mitochondrial dynamics’ is more often applied to the more rapidly changing aspects of mitochondrial shape and organization within a cell. Within all cells, mitochondria exist as a population of organelles undergoing continual fusion into highly branched networks and fission into

A. J. Valente · J. Fonseca · F. Moradi · G. Foran ·  
A. Necakov · J. A. Stuart (✉)  
Department of Biological Sciences, Brock University,  
St. Catharines, ON, Canada  
e-mail: [jstuart@brocku.ca](mailto:jstuart@brocku.ca)

smaller punctate and rod-like structures. The processes of fusion and fission, and their balance or imbalance to bring about remodeling and/or re-localization of mitochondria, are of biological and physiological significance.

The dynamic nature of mitochondria has been appreciated since, over a century ago, Lewis and Lewis [1] noted not only the heterogeneous morphology of mitochondria, but also how that morphology would change over time, morphing from long threadlike structures, to rings, to granules, and back. It was not until 1980, however, that mitochondrial labeling in live cells was demonstrated using rhodamine 123, a dye previously used for lasers [2]. Only a year later it was noted that rhodamine 123 could be used as an indicator of membrane potential as it was lost from the mitochondria of cells treated with uncouplers such as carbonyl cyanide-4-(trifluoromethoxy) phenylhydrazone (FCCP) [3]. This provided the means for probing not only the morphology but also the functional characteristics of mitochondria in live cells. Fluorescence microscopy studies have since benefited from the development of a wide variety of fluorescent small molecule probes and, more recently, fluorescent proteins and genetically encoded sensors. An extensive overview of many of the available mitochondrial labels and probes can be found in [4]. More recently, improvements in the computing technology for working with the large datasets that can be acquired using these methods have enabled significant leaps forward in the analysis of mitochondrial dynamics.

In many human mitochondrial diseases, relative rates of fusion and fission are affected directly via the inheritance of mutations in the genes involved in regulating these processes. In other diseases, such as cancer or diabetes, the connection is indirect but there are reasons to believe that treatment options could be productively targeted to the machinery of mitochondrial dynamics. It is, in general, important to understand how disease processes negatively affect mitochondrial dynamics and how pharmacological interventions might be targeted to correct this. A necessary step toward this goal is the development and refinement of methods for visualizing

and analyzing mitochondria in live cells. In this chapter we focus primarily on fluorescence microscopy approaches for studying the steady-state characteristics of mitochondrial structure and function in live mammalian cells in the contexts of normal and diseased states.

### 10.1.1 Mitochondrial Dynamics in Cell Processes

Within an individual mammalian cell, mitochondria undergo continual structural and positional changes that lead to the highly heterogeneous morphologies we observe under the microscope. Rafelski and colleagues have provided a detailed description of the size, shape, and position of mitochondrial structures that occur [5, 6]. The machinery and molecular mechanisms of mitochondrial fusion/fission have been extensively studied, and readers are directed to several recent reviews for details of these [7, 8].

The overall architecture of mitochondrial networks, including the relative occurrence of punctate or tubular ‘individual’ mitochondrial structures versus highly interconnected and branched structures, represents the balance between fusion and fission processes at a given moment. Fusion and fission processes are in turn mediated by several molecular motors that use the energy in GTP to drive conformational changes. In the outer membrane of mammalian mitochondria, fusion is mediated by the mitofusins (Mfn1, Mfn2), and fission by Drp1. In the inner membrane, Opa1 participates in both fusion and fission processes. A number of accessory proteins interact with this core machinery to facilitate and direct the functions of fusion and fission proteins. Several post-translational modifications have been identified that further refine the functions of Mfn1/2 and Drp1 through changes in protein localization and specific activity [8, 9]. In addition, mitochondria are tethered to cytoskeletal elements and other organelles (e.g. endoplasmic reticulum) [10], and these interactions can influence the distribution and organization of mitochondria within the cell.

Since mitochondria are dynamic organelles, capable of fusion, fragmentation, biogenesis, mitophagy, and intra- or inter-cellular transport, the overall state of the mitochondrial network and its distribution within a cell is fluid. In studies performed in live cells *in vitro*, mitochondrial movement is variable, but can be sufficiently rapid as to interfere with imaging by introducing artifacts where movement rates exceed image acquisition rates. Alternatively, stable features of mitochondrial networks arise that are associated with specific cellular activities. For example, the relative distribution of mitochondria between branched networks and more fragmented individual structures changes over the course of the cell cycle [11]. In addition, metabolic switching from greater reliance on oxidative phosphorylation to glucose fermentation is associated with stable increases in fragmentation and a reduction of overall mitochondrial mass. Mitochondrial network characteristics are also related to cell stress and disease. Relatively rapid (in live cell culture, on the order of minutes) fragmentation of networks can occur when oxidative phosphorylation is uncoupled by protonophores like FCCP, or respiration is inhibited by, for example, hypoxia/anoxia. There are important direct and indirect links between mitochondrial network characteristics and cellular stress and disease. Pharmacological or hormonal targeting of the machinery of mitochondrial dynamics could represent a promising clinical approach to treating symptoms.

### 10.1.2 Mitochondrial Dynamics in Disease

The dynamic morphological characteristics of mitochondrial networks are affected directly and indirectly in many diseases. Peripheral neuronal pathologies are associated with mutations in *Mfn2*, *Opa1*, and various accessory proteins that coordinate the activities of these proteins, consequently affecting mitochondrial dynamics and the steady state morphology of mitochondrial networks. Several recent reviews discuss details of these diseases [12–14]. Barth syndrome,

caused by mutations in the cardiolipin synthase enzyme *Tafazzin*, is characterized by mitochondrial fragmentation, perhaps related to the requirement of critical fusion/fission proteins for cardiolipin [15]. In addition, more indirect links between cellular dysfunctions and mitochondrial network fragmentation have been identified in a growing list of diseases. In cancer cells, where metabolism has shifted toward increased dependence on glycolysis and pentose phosphate pathway activity, mitochondrial networks are typically more fragmented. Pharmacological inhibition of *Drp1* to reduce fission rates can improve the fusion state of mitochondrial networks and slow cancer cell growth [16]. Increased network fragmentation is also observed in neurodegenerative diseases and diabetes. The physiological significance of these observations has not always been established, but in some instances there is evidence that recovery of a highly fused mitochondrial state might improve cell function. There is therefore growing interest in mitochondrial dynamics as a pharmacological target in various diseases, and concomitantly an increasing need to determine the efficacy of putative molecular effectors by quantifying their effects on mitochondrial dynamics and/or steady state network morphology.

---

## 10.2 Fluorescence Microscopy for Studying Mitochondrial Dynamics

### 10.2.1 Fluorescence Microscopy Techniques

A wide range of fluorescence microscopy techniques has been employed for the study of mitochondrial networks. Resolution, acquisition speed, signal, and phototoxicity represent key experimental considerations and no single microscopy system can simultaneously maximize all of these. Therefore, the selection of a fluorescence microscopy modality should be made based on sample characteristics and the goals of the experiment. Here, we will briefly describe typical benefits and drawbacks of

various fluorescence microscopy modalities in the context of different experimental needs.

Adherent mammalian cells are commonly used to study mitochondrial physiology. These cells exhibit a relatively flat morphology, only a few microns thick. For such thin samples, and many experimental contexts, conventional brightfield fluorescence microscopy is sufficient. Due to the contributions of out of focus light, conventional brightfield microscopy does not lend itself to three-dimensional imaging without further processing, but this can be accomplished by computational means. Deconvolution is used to redistribute photon signals to their correct origins, typically by using some information about the microscope's intrinsic characteristics that determine how the image is distorted.

All optical systems introduce some distortion and degradation of the real image. This leads to the notion of *diffraction limited imaging*, a topic we will return to later. The degradation of an image from acquisition may be described by the convolution of the original image and noise associated with the fluorescence,  $I_d + n_f$ , with the instrument response function or *point spread function*,  $P$ , and the addition of detection noise,  $n_d$ , as follows:

$$I_d = (I_o + n_f) \otimes P + n_d$$

The goal of deconvolution is to restore the true image,  $I_o$ , from the acquired dataset. As the point spread function is a three-dimensional entity, best results are obtained from deconvolving three-dimensional stacks with a three-dimensional empirical or theoretical point spread function. There are numerous reviews and book chapters devoted to describing the deconvolution approaches used in practice [17–19]. For thicker samples, or more highly light-scattering samples, such as the mitochondria densely packed about lipid droplets typical in adipocytes, deconvolution brightfield microscopy may be insufficient to fully resolve the structures of interest. In these cases, alternative means for acquiring optical sections may be essential.

Confocal microscopy, both laser scanning and spinning disk, provides a physical solution for

excluding out of focus light from collected images to generate optical sections. The reader is directed to The Handbook of Biological Confocal Microscopy [20] and several book chapters and reviews [21–23] for in depth information regarding confocal microscopy and its application. Briefly, a high intensity light source, almost exclusively a laser, is used to excite a small volume of the sample. Fluorescence is collected while excluding out of focus photons by introducing a confocal aperture between the detector and sample. In laser scanning confocal systems this sampling volume is raster scanned across the sample while recording the fluorescence intensity with a point detector such as a photomultiplier tube, to generate an image one pixel at a time. Spinning disk systems generate a set of independent sampling volumes that are simultaneously scanned and detected on an area detector (typically a CMOS or electron multiplying CCD) to build up an image in a fraction of the time as needed for scanning. While scanning a single point at a time inherently results in longer acquisition times, it provides the ability to selectively bleach or photo-activate regions. For dynamic experiments such as fluorescence recovery after photobleaching or photoactivation of optogenetic constructs, such control is beneficial if not mandatory. Due to the physical rejection of a large portion of emitted photons, confocal methods typically use higher intensity excitation light which may result in greater phototoxicity and sample degradation.

Optical sectioning can be achieved post-acquisition as well by modulating the illumination pattern on the sample. This is referred to as optical sectioning structured illumination microscopy (OS-SIM), not to be confused with super-resolution structured illumination microscopy (SR-SIM). Recovery of optical sections by structured illumination was described as early as 1997 [24]. Such systems work by projecting a structured pattern, typically a regular grid, onto a specimen which causes only the in focus regions to be efficiently illuminated. By stepping the grid position through the full sample, each position in the image is sampled both efficiently and inefficiently allowing for the contri-

butions of out of focus fluorescence to be effectively discarded. The Zeiss Apotome system provides this functionality in a commercially available package that has been shown to provide resolution comparable to or better than confocal methods, though with reduced performance on thicker samples [25]. These systems provide a performant alternative to confocal microscopy, especially for thin samples such as adherent mammalian cells.

The methods of image acquisition discussed above are diffraction-limited. With growing interest in mitochondrial morphology and automated morphological analysis, there has been a need for higher resolution techniques, especially for more difficult compact morphologies. Super-resolution fluorescence microscopy is the blanket term for many techniques that can generate images exceeding the theoretical maximum resolution for a microscope, approximately  $\frac{1}{2}$  the wavelength of light being imaged with or typically about 200–300 nm. Some systems rely primarily on hardware to overcome this limit, such as the beam shaping of stimulated emission depletion (STED) microscopy [26], or the multi-lens arrangement of a  $4\pi$  microscope [27]. Other systems use a combination of hardware and software to reconstruct images at a higher resolution than would otherwise be possible. Such systems include SR-SIM [28], photoactivatable probe localization based techniques including stochastic optical reconstruction microscopy (STORM) [29] and photoactivatable localization microscopy (PALM) [30]. These methods can provide resolution ranging from roughly 100 nm down to tens of nm in the case of localizing methods. There is benefit in such high-resolution techniques, but there are also some drawbacks associated with acquisition and image characteristics. Super-resolution methods often mandate either high intensity illumination, long acquisition periods, or both. This can be a serious drawback for imaging live cells as high resolution becomes irrelevant if there is movement artifact or phototoxicity effects. This typically limits the practicality of such techniques to fixed samples, though there have been several notable live cell examples [31–35].

Motivated by the need for fast, high resolution, and gentle fluorescence microscopy techniques, light sheet microscopy, or selective plane illumination microscopy (SPIM), has been gaining more attention. There are many examples of how light sheet microscopy has already proven itself as an important tool for live imaging of larger samples [36]. Light sheet imaging is typically thought of as a performant method for imaging larger samples at cellular resolution while limiting phototoxicity by only illuminating the focal plane. However, it can be implemented to generate thinner light sheets using Bessel beams and has been demonstrated as a tool for imaging live cells with resolution similar to confocal techniques but while capturing over 100 frames/s [37]. As the resolution of light sheet microscopy is continuously improved, its ability to acquire 3D datasets at astonishing rates while remaining relatively gentle to the sample will likely stimulate the adoption of this technique for the study of mitochondrial dynamics.

## 10.2.2 Experimental Considerations

In live cell imaging, it is essential to maintain temperature and CO<sub>2</sub> levels, and minimize photo-damage during acquisition. To illustrate this, we have provided results from time lapse videos of mitochondria in cells under conditions in which these variables are not controlled. Profound changes in mitochondrial networks occur rapidly (<10 min) when cell culture dishes are shifted from incubators to atmosphere when bicarbonate is a major media pH buffer (Fig. 10.1). Therefore, on-stage maintenance of CO<sub>2</sub>, or use of media insensitive to CO<sub>2</sub> changes is a critical feature of a microscopy system used for mitochondrial imaging in live cells. Intense light exposure can also lead to mitochondrial damage and rapid morphological changes [33], eventually leading to cell death. Assessing phototoxicity, minimizing sample damage, and optimizing acquisition parameters are non-trivial tasks but essential for live cell investigations [38]. Ensuring samples are “happy” on the stage can be difficult, but a practical start to assessing their tolerance of



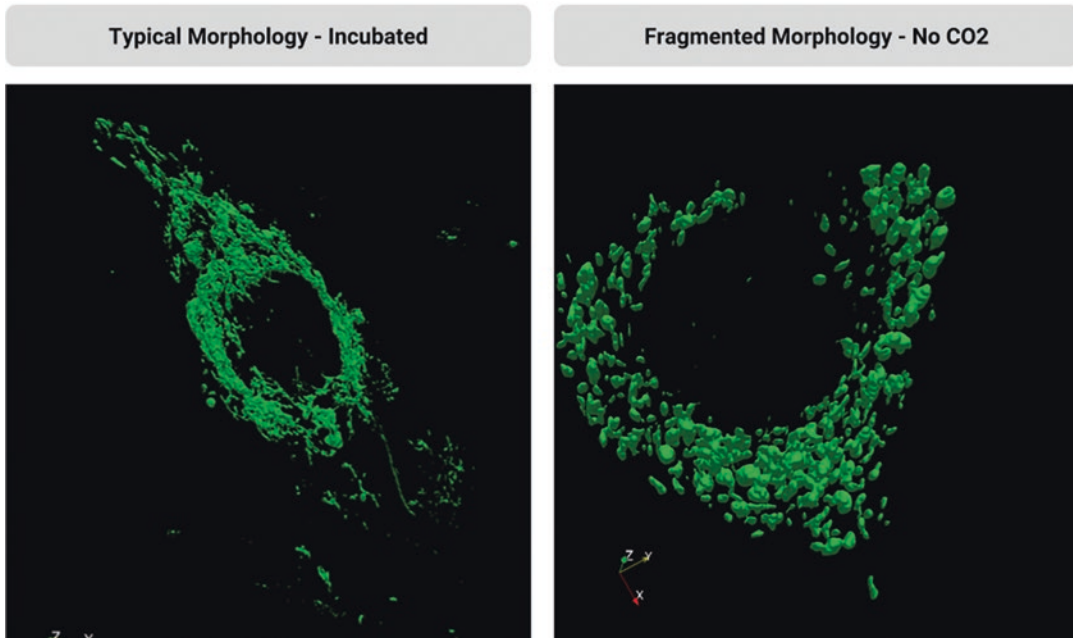


**Fig. 10.1 Morphological changes induced by sub-optimal environmental control during image acquisition.** C2C12 and PC3 cells stably transfected with mEmeral-Mito-7 (a gift from Michael Davidson, Florida State University) were grown in Dulbecco's Modified Eagle Medium (DMEM) supplemented with 10% fetal bovine serum (FBS) in a humidified 5% CO<sub>2</sub> atmosphere at 37 °C. Live cell fluorescence images were obtained with a Plan-Apochromat 63×/1.40 Oil DIC M27 microscope objective using a Carl Zeiss Axio Observer Z1 inverted light/epifluorescence microscope equipped with ApoTome.2 optical sectioning and a Hamamatsu ORCA-Flash 4.0 V2 digital camera. The microscope stage and objectives were maintained at 37 °C, with temperature

control achieved through TempModule S-controlled stage heater and objective heater (PeCon, Erbach, Germany). CO<sub>2</sub> was maintained for the left image, while the right image was taken without any gas regulation on stage. Green fluorescence was detected using a fluorescence channel possessing excitation and emission wavelength filter sets of 450–490 nm and 500–550 nm, respectively. Both the intensity of fluorescence illumination and camera exposure time were held constant throughout all experiments. Z-stacks consisted of 20 slices, each 0.25 μm apart and used to produce 3D renderings using Fiji and ParaView. Cells imaged without CO<sub>2</sub> regulation demonstrate significantly altered morphology from those cells imaged under 5% CO<sub>2</sub>

specific experimental conditions is to image control samples over a duration longer than that of the experiment and note if any cellular or organelle morphological changes appear outside of what one might expect.

A less appreciated aspect of experimental design in studies of mitochondrial networks in live cells is the importance of two other media constituents: oxygen and glucose. If the goal of an experiment is to model *in vivo* conditions, then 1–6% O<sub>2</sub> and 5 mM glucose [39] are appropriate near-physiological levels for most cell types. Glucose has been shown to affect mitochondrial morphology significantly. Under hyperglycemic conditions (20 mM glucose),

mitochondrial morphology appears fragmented unlike the typically fused mitochondria in low glucose (5 mM) culture [40], a more physiologically relevant condition. Furthermore, measuring fusion by determining the extent of locally photo-activated photo-activatable GFP dispersion [41] demonstrates a reduction in fusion associated with high glucose conditions [40]. Provided that the mitochondria appear to behave vastly different under different nutrient loads, this is likely an important consideration in designing experiments investigating the mitochondrial implications of a compound or treatment.

We routinely use 5% O<sub>2</sub> as a physiologically relevant O<sub>2</sub> setpoint and have found that cellular

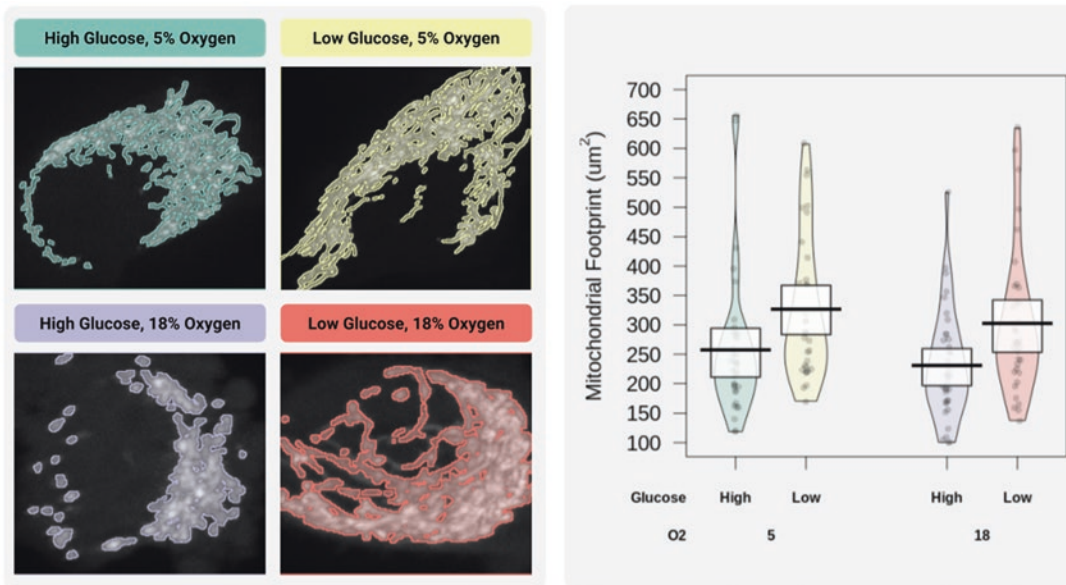


**Fig. 10.2 Media oxygen and glucose levels affect mitochondrial morphology.** C2C12 and PC3 cells stably transfected with mEmeral-Mito-7 (a gift from Michael Davidson, Florida State University) were grown in Dulbecco's Modified Eagle Medium (DMEM) supplemented with 10% fetal bovine serum (FBS) in a humidified 5% CO<sub>2</sub> atmosphere at 37 °C. O<sub>2</sub> levels in the incubators were maintained at either 5% or 18%. Glucose concentrations in DMEM were either 5 mM (low) or 25 mM (high). Cells were grown for 48 h in each condition and each condition was maintained throughout imaging. Live cell fluorescence images were obtained with a Plan-Apochromat 63×/1.40 Oil DIC M27 microscope objective using a Carl Zeiss Axio Observer Z1 inverted light/epifluorescence microscope equipped with ApoTome.2 optical sectioning and a Hamamatsu ORCA-Flash 4.0 V2 digital camera. The microscope stage and objectives were maintained at 37 °C, with temperature

control achieved through TempModule S-controlled stage heater and objective heater (PeCon, Erbach, Germany). Green fluorescence was detected using a fluorescence channel possessing excitation and emission wavelength filter sets of 450–490 nm and 500–550 nm, respectively. Both the intensity of fluorescence illumination and camera exposure time were held constant throughout all experiments. Z-stacks consisted of 20 slices, each 0.25 µm apart and used to produce maximum intensity projections using Fiji. Mitochondrial footprint was determined by generating a binary mask using an automatically determined threshold via Otsu's method within Fiji following noise filtering by a median filter of radius 2 pixels and sharpened with an unsharp mask with a 2 pixel radius and 0.6 strength. The area measures are presented as pirate plots where each data point is plotted as a point, the boxes represents the 95% confidence intervals, the dark lines are the means, and the coloured bean is the density. Plots were generated using the yarr package for R

reactive oxygen species (ROS) production, specifically hydrogen peroxide, is greater at 18% O<sub>2</sub>, at which most cell culture is done. Since mitochondrial dynamics may be affected by intracellular ROS, it will in most instances be inappropriate to use 18% O<sub>2</sub> as a control for experimental comparisons. Figure 10.2 shows how continual exposure for >48 h to 5% or 18% O<sub>2</sub> affects two mitochondrial network parameters: network size (number of branches per network) and mitochondrial footprint (total area per cell in a compressed z-stack image occupied by mitochondria). Similar effects are observable on

other mitochondrial morphological parameters (not shown here). Note that the effects of O<sub>2</sub> and glucose on mitochondrial morphology might be difficult to predict, as evidenced by the fact that they are not consistent between the two cell types studied here. Glucose effects are equally significant. Most eukaryotic cells in culture respond to low (physiological; 5 mM) glucose levels by increasing their reliance on oxidative phosphorylation to generate ATP, and this can increase the mitochondrial footprint (Fig. 10.2). If the goal of an experiment is to identify small molecules that can alter mitochondrial network morphology

in vivo, then it may be critical to begin with the more extensive and fused network associated with physiological levels of  $O_2$  and glucose.

### 10.2.3 Analyzing Mitochondrial Morphology in Micrographs

With the plethora of mitochondrial probes, variety of fluorescence microscopy systems, and continually improving computer processing and data storage solutions, it is no surprise how prominent live cell fluorescence microscopy has become in mitochondrial research. Having hundreds or thousands of individual cells imaged can be very powerful, but only if morphology and function can be compared efficiently and reliably. There are numerous open source platforms for image analysis available, such as Fiji [42], CellProfiler [43], and scikit-image [44]. Tools such as these have provided the means for generating transparent, efficient, and shareable methods.

The most basic analysis of morphology is to merely qualitatively assign descriptive keywords to images or groups - terms like fused, fragmented, and intermediate. It is easy to unintentionally introduce confirmation bias through such an analysis. This is not an issue unique to microscopy and there are ways to improve the faithfulness of such analyses. Blind analysis helps to reduce the injection of bias into qualitative observations, and its implementation may be as simple as removing identifying labels and scrambling image analysis order such that the observer is unaware of its experimental group assignment [45]. When deciding on how to classify images, keep in mind that using many categories may help capture more subtle differences, but may also hinder reproducibility. While you may find good agreement between the assignment of a couple of labels (perhaps fragmented and fused), there may be more variation between the results from different observers as more categories are introduced (such as intermediate, swollen, punctate, etc.). Blinding can be done by hand, but there are many tools available. A quick search in a browser for “ImageJ Blind Experiment” or “ImageJ Blind Analysis” will return many useful

tools for doing this in ImageJ that are freely available.

Manual blinded qualitative analysis has its benefits: it is conceptually simple, trivial to explain, and is less susceptible to generating erroneous results due to sub-optimal tuning of analysis parameters or poor image quality. However, it does not allow for efficiently analyzing large datasets like those produced by plate readers and automated microscopy systems. Additionally, it limits the granularity of comparisons to a small number of qualitative bins. To get around these limitations, researchers have developed methods for automated analysis. As described by Harwig et al., approaches can largely be described as morphometric or morphological [4]. Morphometric methods are used to automatically calculate descriptive measures such as areas, perimeters, and lengths [4, 46–54], while morphological methods use this information to bin independent structures or even pixels into qualitative categories [55–60].

Automated analysis methods often follow a similar workflow. First, images are typically pre-processed to enhance contrast and reduce spurious noise. Then, images are segmented such that the signal from the mitochondrial label is separated from the background to produce a binary image. The binary representation can be used to gather various measurements for each spatially independent object or further simplified into a topological skeleton to extract topological information. A topological skeleton is a 1 pixel wide wire frame depiction of segmented structures that can be converted to a set of line segments. The skeleton provides access to measures of length and organizational parameters like the number of branching points. Morphometric approaches either hand the values acquired at this stage back over to the user or summarize them before handing them over to the user. Morphological approaches go a step further. They use the information generated to bin the structures as having one of several categorical morphologies. This is often achieved using supervised machine learning methods such as random forest classifiers or support vector



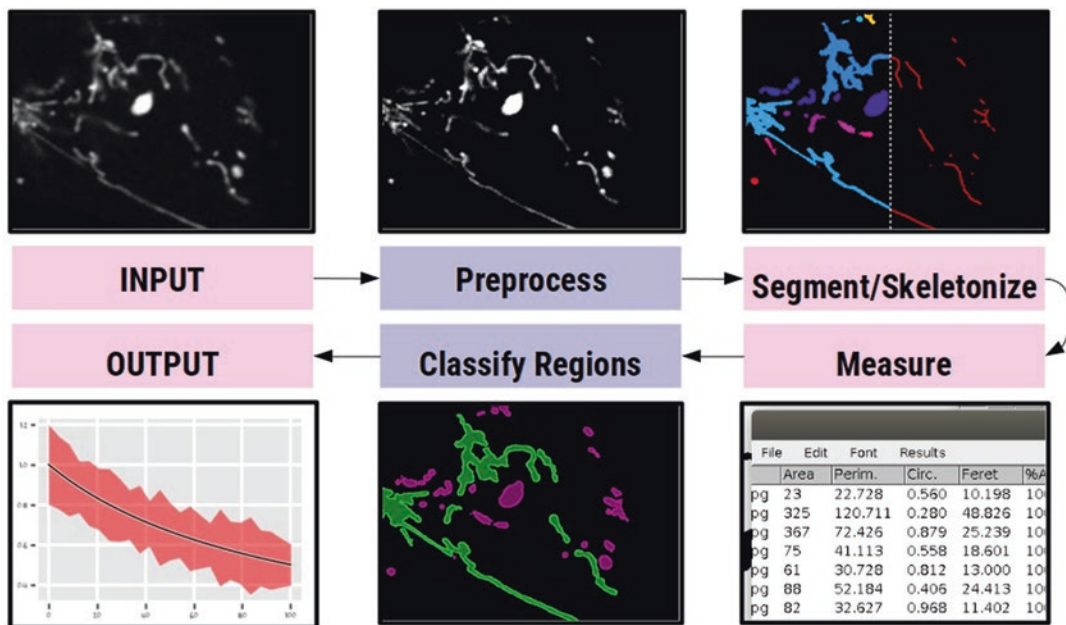


**Fig. 10.3** Morphological analysis typically follows a similar foundational recipe. First an input image is pre-processed to reduce spurious noise and enhance contrast. Then the mitochondria are segmented using a global or local threshold. This binary representation may be further simplified into a skeleton for topological analysis. Various morphometric parameters are then extracted from the

independent regions of the binary and skeletal representations. These may be used for classifying the structures categorically often using supervised learning methods as is typical of morphological binning approaches. Finally, the information is summarized and provided to the user as output for further exploration and statistical analysis

machines. An overview of the generic workflow for analysis is summarized by Fig. 10.3.

Multiple processing methods have additionally sought to address the dynamic nature of mitochondria. Inspection of organizational changes has previously been addressed using colocalization and optical flow measurements. Colocalization between frames has been used as an effective comparison of which regions have or have not changed over time [47, 53]. A perfect correlation indicates no changes have occurred, while a poor correlation indicates more movement is taking place. The movement may arise from fission, fusion, or mitochondria being shuttled throughout the cell. However, it may also arise from the cell itself moving. To compensate for this, a rigid registration may be suitable to pre-align the cell from frame to frame before performing the colocalization. However, this may not fully compensate for more subtle changes in cell shape. An alternative for capturing changes

to the mitochondrial ultrastructure over time is estimation of optical flow [53]. Optical flow estimation aims to measure motion in a series of images as a field of displacement and velocity vectors. The optical flow estimate is beneficial in that it also provides information regarding the directionality of the movements. Both colocalization and optical flow estimation provide a means to assess mitochondrial mobility and are demonstrated in Fig. 10.4. Such methods do not directly address whether fission or fusion is occurring, but rather changes in the organization of mitochondrial structures. Addressing such processes as fission and fusion requires additional methodologies.

To detect fission and fusion events, Westrate et al. tracked independent regions from frame to frame in time series data sets [56]. If two regions merged to generate a single region, a fusion event was recorded, while if a single region broke into two regions a fission event was recorded. This

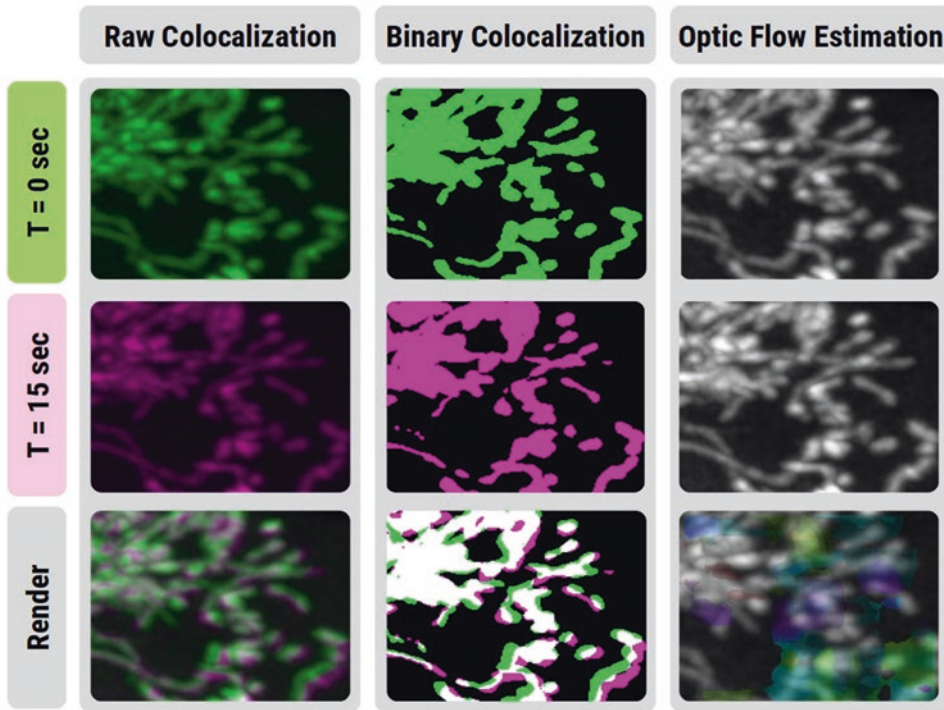


**Fig. 10.4** Besides morphology, there is interest in generating information regarding the movement of mitochondrial objects in cells. This has been investigated using colocalization and optic flow estimation. Here, an example is provided for rendering colocalization and direction maps. In a colocalization, subsequent frames can be coloured green and magenta to produce white where there

is colocalization of signal. Note that colocalizations are not limited to the limiting channel merge technique, but that actual coefficients describing the frame to frame colocalization can be obtained and used as a metric for motility. In the render of optical flow, overlaid above the mitochondrial mitograph, the hue indicates the direction of motion and the brightness the velocity

was done using a scoring system that interpreted the merging or separation of regions as fission or fusion events, respectively. It is important to note that an observation of fission may be made from adjacent mitochondria moving away from each other, or fusion events detected when separated mitochondria clump together without actually fusing. Using well isolated mitochondria and validating connectivity changes by photoactivatable probes as these authors did helps to prevent possible erroneous interpretations [56].

Many of the methods implemented as scripts, extensions, macros, or plugins are publicly and freely available. A summary of these available methodologies has been summarized in Table 10.1. As some of these tools, such as MitoGraph and MiNA, are regularly and publicly updated with new features and bug fixes, it is best

to check their respective websites for the most up to date functionality.

The analysis methods published to date all have strengths and weaknesses. The heterogeneity of mitochondrial morphology and organization, variation in image characteristics (such as resolution and noise) from different acquisition systems, and labeling efficacy can all affect the accuracy of an automated analysis method without further tuning. It is important that researchers validate methods for their use. Typically, representative validation images depicting segmentation, classification, or morphological skeleton results should be included in publication, at least as supplementary information. Having projects that are open source and invite collaboration, such as those hosted as GitHub repositories, are helping bring limitations to light by providing an

**Table 10.1** Publicly available methods and their currently demonstrated functionality. Note that time course analysis capability indicates functionality beyond repeated measures at multiple time points

Publication	Availability	2D	3D	Time Course	High Throughput	Functional
Quantitative analysis of mitochondrial morphology and membrane potential in living cells using high-content imaging machine learning and morphological binning – Anthony P. Leonard <i>et al.</i> , 2015	Supplementary	✓			✓	✓
Multiplexed high-content analysis of mitochondrial morphofunction using live-cell microscopy – Eligio F. Iannetti <i>et al.</i> , 2016	Supplementary	✓			✓	✓
Loss of PINK1 Function Promotes Mitophagy through Effects on Oxidative Stress and Mitochondrial Fission – Ruben K. Dagda <i>et al.</i> , 2009	<a href="http://imagejdocu.tudor.lu/doku.php?id=plugin:morphology:mitochondrial_morphology_macro Plug-in:start">http://imagejdocu.tudor.lu/doku.php?id=plugin:morphology:mitochondrial_morphology_macro Plug-in:start</a>	✓				✓
MitoLoc: A method for the simultaneous quantification of mitochondrial network morphology and membrane potential in single cells - Jakob Vowinckel <i>et al.</i> , 2015	<a href="https://www.gurdon.cam.ac.uk/institute-life/downloadspublic/imaging-plugins">https://www.gurdon.cam.ac.uk/institute-life/downloadspublic/imaging-plugins</a>		✓			✓
A novel algorithm identifies stress-induced alterations in mitochondrial connectivity and inner membrane structure from confocal images - Mathieu Ouellet <i>et al.</i> , 2017	<a href="http://www.uqtr.ca/LaboMarcGermain">http://www.uqtr.ca/LaboMarcGermain</a>	✓				
Methods for imaging mammalian mitochondrial morphology: A prospective on MitoGraph - Megan Cleland Harwig <i>et al.</i> , 2018	<a href="https://github.com/vianamp/MitoGraph">https://github.com/vianamp/MitoGraph</a>	✓	✓			
MyToe: automatic analysis of mitochondrial dynamics – Eero Lihavainen <i>et al.</i> , 2012	<a href="http://www.cs.tut.fi/~sanchesr/tool_MyToe/MyToe.html">http://www.cs.tut.fi/~sanchesr/tool_MyToe/MyToe.html</a>	✓		✓		
A simple ImageJ macro tool for analyzing mitochondrial network morphology in mammalian cell culture – Valente <i>et al.</i> , 2017	<a href="https://github.com/StuartLab/MINA">https://github.com/StuartLab/MINA</a>	✓				

For example, motion analysis through inter-frame colocalization or optical flow would be considered time course functionalities. High throughput analysis indicates demonstration for use with slide scanners or high content imaging systems and functional capabilities include things such as membrane potential probe quantification

avenue for dialog and action to improve methods and the general usefulness of these tools.

### 10.3 Conclusions and Future Perspectives

The past decade has seen significant progress in our understanding of mitochondrial dynamics in the context of various disease states. Much of this relates to the identification of the proteins that mediate fusion and fission. There is still much progress to be made in refining the methods used to analyze specific aspects of mitochondrial dynamics. We have shown here the importance of maintaining temperature, CO<sub>2</sub>, O<sub>2</sub>, and glucose levels to avoid the introduction of artifactual effects on mitochondrial network morphology. Similarly, virtually all of the tools used to fluorescently label mitochondria in live cells can, under some circumstances, induce artifactual changes in mitochondrial form and function, so it is important to consider and appropriately control

for these. Also, the very act of exposing cells to large quantities of light may induce cellular responses not relevant to in vivo physiology, so it is important to design experimental protocols with the goal of avoiding phototoxicity.

Once having obtained high quality data from well controlled and calibrated experiments, a variety of tools has been developed to support qualitative and/or quantitative analyses (Table 10.1). One advantage of using such tools is the avoidance of cognitive bias in the analysis of results. Mitochondrial network analysis tools such as those described in Table 10.1 take steps to formalize the specific parameters of interest being measured and provide summary statistics in a relatively objective way. Many of these tools have been provided as open source code to promote their continued refinement and development. These tools can be combined with high-throughput approaches for identifying small molecules that improve mitochondrial function in disease. While important developments in electron microscopic tomography have

provided finer detail of mitochondrial structure, this approach requires fixing cells and generates relatively large datasets that are not conducive to high-throughput analyses. Thus, live cell fluorescence microscopy combined with a formally defined analysis that can be reproduced by others represents an effective compromise between resolution and attainability for the study of mitochondrial network morphology in disease.

One of the more exciting recent developments in mitochondrial research is the development of novel Optogenetic approaches that allow for precise spatio-temporal control of discrete mitochondrial functions. These include light-gated control of protein localization to the outer mitochondrial membrane [57–60], control of endoplasmic reticulum-mitochondria tethering [61], control of mitochondrial metabolism and  $\text{Ca}^{2+}$  signaling [62], inactivation of mitochondrial electron transport chain complex II [63], and guided localization of mitochondria to discrete subcellular regions [64–67]. These approaches lend themselves to live cell fluorescence imaging of mitochondria and will dovetail naturally with computational approaches for subsequent analysis. Together, these new tools promise to push the field toward a deeper and more complete understanding of mitochondrial dynamics in health and disease.

## References

- Lewis MR, Lewis WH (1914) Mitochondria in tissue culture. *Science* 39:330–333
- Johnson LV, Walsh ML, Chen LB (1980) Localization of mitochondria in living cells with rhodamine 123. *Proc Natl Acad Sci U S A* 77:990–994
- Johnson LV (1981) Monitoring of relative mitochondrial membrane potential in living cells by fluorescence microscopy. *J Cell Biol* 88:526–535
- Harwig MC, Viana MP, Egner JM, Harwig JJ, Widlansky ME, Rafelski SM et al (2018) Methods for imaging mammalian mitochondrial morphology: a prospective on MitoGraph. *Anal Biochem* 552:81–99
- Rafelski SM, Marshall WF (2008) Building the cell: design principles of cellular architecture. *Nat Rev Mol Cell Biol* 9:593–602
- Rafelski SM (2013) Mitochondrial network morphology: building an integrative, geometrical view. *BMC Biol* 11:71
- Tilokani L, Nagashima S, Paupe V, Prudent J (2018) Mitochondrial dynamics: overview of molecular mechanisms. *Essays Biochem* 62:341–360
- Yu SB, Pekkurnaz G (2018) Mechanisms orchestrating mitochondrial dynamics for energy homeostasis. *J Mol Biol* 430(21):3922–3941. <https://doi.org/10.1016/j.jmb.2018.07.027>
- Cid-Castro C, Hernández-Espinosa DR, Morán J (2018) ROS as regulators of mitochondrial dynamics in neurons. *Cell Mol Neurobiol* 38:995–1007
- Schorr S, van der Laan M (2018) Integrative functions of the mitochondrial contact site and cristae organizing system. *Semin Cell Dev Biol* 76:191–200
- Rambold AS, Lippincott-Schwartz J (2011) Mechanisms of mitochondria and autophagy crosstalk. *Cell Cycle* 10:4032–4038
- Pareyson D, Saveri P, Sagnelli A, Piscoquito G (2015) Mitochondrial dynamics and inherited peripheral nerve diseases. *Neurosci Lett* 596:66–77
- Bagli E, Zikou AK, Agnantis N, Kitsos G (2017) Mitochondrial membrane dynamics and inherited optic neuropathies. *In Vivo* 31:511–525
- Filadi R, Pendin D, Pizzo P (2018) Mitofusin 2: from functions to disease. *Cell Death Dis* 9:330
- Kameoka S, Adachi Y, Okamoto K, Iijima M, Sesaki H (2018) Phosphatidic acid and cardiolipin coordinate mitochondrial dynamics. *Trends Cell Biol* 28:67–76
- Rehman J, Zhang HJ, Toth PT, Zhang Y, Marsboom G, Hong Z et al (2012) Inhibition of mitochondrial fission prevents cell cycle progression in lung cancer. *FASEB J. Federation of American Societies for Experimental Biology Bethesda, MD, USA* 26:2175–2186
- Sarder P, Nehorai A (2006) Deconvolution methods for 3-D fluorescence microscopy images. *IEEE Signal Process Mag* 23:32–45
- Goodwin PC (2014) Quantitative deconvolution microscopy. *Methods Cell Biol* 123:177–192
- Biggs DSC (2010) 3D Deconvolution Microscopy. *Curr Protoc Cytom* 52:12.19.1–12.19.20
- Pawley J (2010) Handbook of biological confocal microscopy. Springer Science & Business Media, New York
- Conchello J-A, Lichtman JW (2005) Optical sectioning microscopy. *Nat Methods* 2:920–931
- Gräf R, Rietdorf J, Zimmermann T (2005) Live cell spinning disk microscopy. *Adv Biochem Eng Biotechnol* 95:57–75
- Paddock SW, Eliceiri KW (2013) Laser scanning confocal microscopy: history, applications, and related optical sectioning techniques. *Methods Mol Biol* 1075:9–47
- Neil MA, Juskaitis R, Wilson T (1997) Method of obtaining optical sectioning by using structured light in a conventional microscope. *Opt Lett* 22:1905–1907
- Weigel A, Schild D, Zeug A (2009) Resolution in the ApoTome and the confocal laser scanning microscope: comparison. *J Biomed Opt* 14:014022
- Hell SW, Wichmann J (1994) Breaking the diffraction resolution limit by stimulated emission: stimulated-emission-depletion fluorescence microscopy. *Opt Lett* 19:780



27. Hell SW, Stelzer EHK, Lindek S, Cremer C (1994) Confocal microscopy with an increased detection aperture: type-B 4Pi confocal microscopy. *Opt Lett, OL Optical Soc Am* 19:222–224
28. Gustafsson MGL (2000) Surpassing the lateral resolution limit by a factor of two using structured illumination microscopy. *SHORT COMMUNICATION. J Microsc* 198:82–87
29. Rust MJ, Bates M, Zhuang X (2006) Sub-diffraction-limit imaging by stochastic optical reconstruction microscopy (STORM). *Nat Methods* 3:793–796
30. Hess ST, Girirajan TPK, Mason MD (2006) Ultra-high resolution imaging by fluorescence photoactivation localization microscopy. *Biophys J* 91:4258–4272
31. Fiolka R, Shao L, Rego EH, Davidson MW, Gustafsson MGL (2012) Time-lapse two-color 3D imaging of live cells with doubled resolution using structured illumination. *Proc Natl Acad Sci U S A* 109:5311–5315
32. Shao L, Kner P, Rego EH, Gustafsson MGL (2011) Super-resolution 3D microscopy of live whole cells using structured illumination. *Nat Methods* 8:1044–1046
33. Shim S-H, Xia C, Zhong G, Babcock HP, Vaughan JC et al (2012) Super-resolution fluorescence imaging of organelles in live cells with photoswitchable membrane probes. *Proc Natl Acad Sci* 109:13978–13983
34. Gugel H, Bewersdorf J, Jakobs S, Engelhardt J, Storz R, Hell SW (2004) Cooperative 4Pi excitation and detection yields sevenfold sharper optical sections in live-cell microscopy. *Biophys J* 87:4146–4152
35. Egner A, Jakobs S, Hell SW (2002) Fast 100-nm resolution three-dimensional microscope reveals structural plasticity of mitochondria in live yeast. *Proc Natl Acad Sci U S A* 99:3370–3375
36. Ahrens MB, Orger MB, Robson DN, Li JM, Keller PJ (2013) Whole-brain functional imaging at cellular resolution using light-sheet microscopy. *Nat Methods* 10:413–420
37. Planchon TA, Gao L, Milkie DE, Davidson MW, Galbraith JA, Galbraith CG et al (2011) Rapid three-dimensional isotropic imaging of living cells using Bessel beam plane illumination. *Nat Methods* 8:417–423
38. Laissue PP, Alghamdi RA, Tomancak P, Reynaud EG, Shroff H (2017) Assessing phototoxicity in live fluorescence imaging. *Nat Methods* 14:657–661
39. Güemes M, Rahman SA, Hussain K (2016) What is a normal blood glucose? *Arch Dis Child* 101:569–574
40. Liesa M, Shirihi OS (2013) Mitochondrial dynamics in the regulation of nutrient utilization and energy expenditure. *Cell Metab* 17:491–506
41. Twig G, Graf SA, Wikstrom JD, Mohamed H, Haigh SE, Elorza A et al (2006) Tagging and tracking individual networks within a complex mitochondrial web with photoactivatable GFP. *Am J Physiol Cell Physiol* 291:C176–C184
42. Schindelin J, Arganda-Carreras I, Frise E, Kaynig V, Longair M, Pietzsch T et al (2012) Fiji: an open-source platform for biological-image analysis. *Nat Methods Nat Publ Group* 9:676
43. Lamprecht MR, Sabatini DM, Carpenter AE (2007) CellProfiler: free, versatile software for automated biological image analysis. *Biotechniques* 42:71–75
44. van der Walt S, Schönberger JL, Nunez-Iglesias J, Boulogne F, Warner JD, Yager N et al (2014) scikit-image: image processing in python. *PeerJ* 2:e453
45. MacCoun R, Perlmutter S (2015) Blind analysis: Hide results to seek the truth. *Nature* 526:187–189
46. Iannetti EF, Smeitink JAM, Beyrath J, Willems PHGM, Koopman WJH (2016) Multiplexed high-content analysis of mitochondrial morphofunction using live-cell microscopy. *Nat Protoc* 11:1693–1710
47. Koopman WJH, Visch H-J, Smeitink JAM, Peter HG (2005) Simultaneous quantitative measurement and automated analysis of mitochondrial morphology, mass, potential, and motility in living human skin fibroblasts. *Cytometry A* 69A:1–12
48. Nikolaisen J, Nilsson LIH, Pettersen IKN, Peter HG, Lorens JB, Koopman WJH et al (2014) Automated quantification and integrative analysis of 2D and 3D mitochondrial shape and network properties. *PLoS One* 9:e101365
49. Dagda RK, Cherra SJ 3rd, Kulich SM, Tandon A, Park D, Chu CT (2009) Loss of PINK1 function promotes mitophagy through effects on oxidative stress and mitochondrial fission. *J Biol Chem* 284:13843–13855
50. Vowinckel J, Hartl J, Butler R, Ralser M (2015) MitoLoc: a method for the simultaneous quantification of mitochondrial network morphology and membrane potential in single cells. *Mitochondrion* 24:77–86
51. Ouellet M, Guillebaud G, Gervais V, St-Pierre DL, Germain M (2017) A novel algorithm identifies stress-induced alterations in mitochondrial connectivity and inner membrane structure from confocal images. *PLoS Comput Biol* 13:e1005612
52. Viana MP, Lim S, Rafelski SM (2015) Quantifying mitochondrial content in living cells. *Methods Cell Biol* 125:77–93
53. Lihavainen E, Mäkelä J, Spelbrink JN, Ribeiro AS (2012) Mytoe: automatic analysis of mitochondrial dynamics. *Bioinformatics* 28:1050–1051
54. Valente AJ, Maddalena LA, Robb EL, Moradi F, Stuart JA (2017) A simple ImageJ macro tool for analyzing mitochondrial network morphology in mammalian cell culture. *Acta Histochem* 119:315–326
55. Peng J-Y, Lin C-C, Chen Y-J, Kao L-S, Liu Y-C, Chou C-C et al (2011) Automatic morphological subtyping reveals new roles of caspases in mitochondrial dynamics. *PLoS Comput Biol* 7:e1002212
56. Westrate LM, Drocco JA, Martin KR, Hlavacek WS, MacKeigan JP (2014) Mitochondrial morphological features are associated with fission and fusion events. *PLoS One* 9:e95265



57. Milas A, Jagrić M, Martinčić J, Tolić IM (2018) Optogenetic reversible knocksideways, laser ablation, and photoactivation on the mitotic spindle in human cells. *Methods Cell Biol* 145:191–215. <https://doi.org/10.1016/bs.mcb.2018.03.024>. Epub 2018 Apr 26. PubMed PMID: 29957204
58. Wang H, Vilela M, Winkler A, Tarnawski M, Schlichting I, Yumerefendi H, Kuhlman B, Liu R, Danuser G, Hahn KM (2016) LOVTRAP: an optogenetic system for photoinduced protein dissociation. *Nat Methods* 13(9):755–758. <https://doi.org/10.1038/nmeth.3926>. Epub 2016 Jul 18. PubMed PMID: 27427858; PubMed Central PMCID: PMC5137947
59. Wang H, Hahn KM (2016) LOVTRAP: a versatile method to control protein function with light. *Curr Protoc Cell Biol* 73:21.10.1–21.10.14. <https://doi.org/10.1002/cpcb.12>. PubMed PMID: 27906450; PubMed Central PMCID: PMC5137945
60. Valon L, Marín-Llauradó A, Wyatt T, Charras G, Trepast X (2017) Optogenetic control of cellular forces and mechanotransduction. *Nat Commun* 8:14396. <https://doi.org/10.1038/ncomms14396>. PubMed PMID: 28186127; PubMed Central PMCID: PMC5309899
61. Shi F, Kawano F, Park SE, Komazaki S, Hirabayashi Y, Polleux F, Yazawa M (2018) Optogenetic control of endoplasmic reticulum-mitochondria tethering. *ACS Synth Biol* 7(1):2–9. <https://doi.org/10.1021/acssynbio.7b00248>. Epub 2017 Dec 4. PubMed PMID: 29172503
62. Tkatch T, Greotti E, Baranauskas G, Pendin D, Roy S, Nita LI, Wettmarshausen J, Prigge M, Yizhar O, Shirihai OS, Fishman D, Hershfinkel M, Fleidervish IA, Perocchi F, Pozzan T, Sekler I (2017) Optogenetic control of mitochondrial metabolism and Ca<sup>2+</sup> signaling by mitochondria-targeted opsins. *Proc Natl Acad Sci U S A* 114(26):E5167–E5176. <https://doi.org/10.1073/pnas.1703623114>. Epub 2017 Jun 13. PubMed PMID: 28611221; PubMed Central PMCID: PMC5495261
63. Wojtovich AP, Wei AY, Sherman TA, Foster TH, Nehrke K (2016) Chromophore-assisted light inactivation of mitochondrial electron transport chain complex II in *Caenorhabditis elegans*. *Sci Rep* 6:29695. <https://doi.org/10.1038/srep29695>. PubMed PMID: 27440050; PubMed Central PMCID: PMC4954975
64. Cunniff B, McKenzie AJ, Heintz NH, Howe AK (2016) AMPK activity regulates trafficking of mitochondria to the leading edge during cell migration and matrix invasion. *Mol Biol Cell* 27(17):2662–2674. <https://doi.org/10.1091/mbc.E16-05-0286>. Epub 2016 Jul 6. PubMed PMID: 27385336; PubMed Central PMCID: PMC5007087
65. Ballister ER, Aylow S, Chenoweth DM, Lampson MA, Holzbaur ELF (2015) Optogenetic control of organelle transport using a photocaged chemical inducer of dimerization. *Curr Biol* 25(10):R407–R408. <https://doi.org/10.1016/j.cub.2015.03.056>. PubMed PMID: 25989077; PubMed Central PMCID: PMC4737597
66. Duan L, Che D, Zhang K, Ong Q, Guo S, Cui B (2015) Optogenetic control of molecular motors and organelle distributions in cells. *Chem Biol* 22(5):671–682. <https://doi.org/10.1016/j.chembiol.2015.04.014>. Epub 2015 May 9. PubMed PMID: 25963241; PubMed Central PMCID: PMC4443846
67. van Bergeijk P, Adrian M, Hoogenraad CC, Kapitein LC (2015) Optogenetic control of organelle transport and positioning. *Nature* 518(7537):111–114. <https://doi.org/10.1038/nature14128>. Epub 2015 Jan 7. PubMed PMID: 25561173; PubMed Central PMCID: PMC5063096